

## Synthesis of bismuth silicate nanostructures with tunable morphology and enhanced photocatalytic activity

K Karthik, K R Sunaja Devi\* & Dephan Pinheiro

Department of Chemistry, CHRIST (Deemed to be University) Bangalore 560 029, Karnataka, India.

E-mail: sunajadevi.kr@christuniversity.in

Received: 27 September 2018; accepted 4 January 2019

Bismuth oxide due to its narrow bandgap has attracted significant attention as a photocatalyst. A facile and efficient method to synthesize bismuth silicate with tunable morphology and property is achieved in this study. Bismuth oxide and bismuth silicate have been synthesized by surfactant-assisted modified sol-gel method. The fabricated bismuth oxide nanoparticle samples are characterized by various analytical tools such as X-Ray diffractometer, Infra-Red spectroscopy, Scanning Electron microscopy and UV-Diffuse Reflectance spectroscopy. The synthesized nanoparticles exhibit excellent photocatalytic activity for the degradation of Rhodamine B dye in aqueous medium. Bismuth silicate exerts more satisfactory catalytic property and outstanding reusability compared to pure bismuth oxide. The superior stability and enhanced activity enables the application of bismuth silicate as a photocatalyst for environmental remediation.

**Keywords:** Bismuth oxide, Bismuth silicate, Photocatalyst, Rhodamine B, Sol-gel, Surfactant.

Bismuth trioxide ( $\text{Bi}_2\text{O}_3$ ) and modified bismuth oxides have been an area of keen interest due to their unique optical and electrical properties like narrow bandgap, good photoluminescence and photoconductivity properties<sup>1</sup>. Therefore, the semiconductor, bismuth oxide shows varied properties based on their morphology.  $\text{Bi}_2\text{O}_3$  has been studied in the field of solid-state fuel cells, optoelectronics, optical coatings, ceramics, gas sensing and catalysis<sup>2</sup>. As the photocatalytic activity of photocatalysts is influenced by the sizes and morphologies, it is advantageous to fabricate pure and doped bismuth oxide with a controllable morphology that is highly efficient and cost effective<sup>3</sup>.

Pure  $\text{SiO}_2$  was confined mainly to the photocatalytic reactions under UV irradiations like photooxidation of carbon monoxide, photo metathesis and photo epoxidation of alkenes<sup>4-6</sup>. Silicates have been extensively studied in various fields such as catalysis, sensors and as an adsorbent in chromatography. Silicates show poor linearity with high impedance value due to which they haven't gained much attention towards gas sensing applications. Doping metals into silicates is a possible solution to improve the linearity of impedance. Silicates are known to be inert in nature and are inert in various reactions, but they show enhanced activity towards photocatalytic reactions<sup>7</sup>.  $\text{SiO}_2$  has been reported as an active material to enhance

the photocatalytic activity of other semiconducting nanomaterials.  $\text{SiO}_2$  based catalysts such as  $\text{SiO}_2\text{-TiO}_2$ ,  $\text{SiO}_2/\text{Al-TiO}_2$  and  $\text{SiO}_2$  supported  $\text{Cu-TiO}_2$  show high photocatalytic activity under UV and visible light illumination at room temperature<sup>8,9</sup>. These nanoparticles can be used to synthesize new products<sup>10</sup>, for neutralization of hazardous wastes and industrial gas emissions<sup>11</sup>, photocatalytic and photoelectrochemical solar energy transformation<sup>12</sup> and for systems for information storage and transmission<sup>13</sup>.

Rhodamine B (Rh B) is a typical triphenylmethane dye that belongs to xanthene class. Rh B has been used as a food additive but later it got banned due to its carcinogenicity. Paper, dyeing and textile are some of the industries which use Rh B widely in their processes<sup>14</sup>. Rh B is also used as a fluorescent water tracer to detect the ground water<sup>15</sup>. Thus, considering the harmful and hazardous nature of Rh B, it is essential to take some scientific and systematic efforts to remove Rh B from wastewater using photochemical techniques by semiconductor-based photocatalysts.

The objective of this work was to synthesize bismuth silicate nanoparticles, an efficient photocatalyst with a tuneable optical and morphological properties using surfactant mediated sol-gel method. The synthesised photocatalysts were studied for photodegradation of dyes, harmful organic pollutants.

## Experimental Section

### Chemicals

Bismuth nitrate ( $\text{Bi}(\text{NO}_3)_3 \cdot 5\text{H}_2\text{O}$ ), ammonium hydroxide ( $\text{NH}_4\text{OH}$ ), nitric acid ( $\text{HNO}_3$ ), tetraethyl orthosilicate (TEOS), sodium lauryl sulfate (SLS), ethanol and Rhodamine B (Rh B) were purchased from SD fine Chemicals limited (*SDFCL*) and used without purification.

### Synthesis of bismuth oxide and bismuth silicate nanoparticles

$\text{Bi}(\text{NO}_3)_3 \cdot 5\text{H}_2\text{O}$  (9.36 g) was added to distilled water to prepare a solution of the  $\text{Bi}^{3+}$  made acidic by adding concentrated  $\text{HNO}_3$ . TEOS (1.73 g, 10% w/w) and 1 g of SLS were added to the solution of  $\text{Bi}^{3+}$  with stirring at room temperature. A dense white precipitate is formed on addition of ammonium hydroxide to the above solution. The pH of the solution was maintained in alkaline condition for complete precipitation. The solution was stirred continuously to form a sol which on heating resulted in the formation of a white gel. The formed gel was washed with distilled water and finally with ethanol. The gel was dried and calcinated at  $600^\circ\text{C}$  for 4 h in a muffle furnace at a heating of  $10^\circ\text{C}/\text{min}$ . The sample was removed from the furnace after 4 h to arrest the formation of  $\alpha\text{-Bi}_2\text{O}_3$ . The above method was repeated to synthesize bismuth oxide without TEOS under the similar conditions.

### Characterization

The prepared yellow bismuth oxide and bismuth silicate nanoparticles were characterized using powder-XRD, FT-IR and UV-DRS to study the structure and optical properties. XRD patterns were obtained from Bruker AXS Kappa Apex X-ray diffractometer with  $\text{Cu-K}\alpha$  ( $\lambda=1.5406 \text{ \AA}$ ) radiation in the  $2\theta$  range of  $5 - 90^\circ$ . The lattice constants were determined using *Match* software. The surface morphology of the powder was observed using a FEI Inspect S50- Scanning electron microscope (SEM). The optical studies were carried out with a diffuse reflectance spectrophotometer (DRS), using Shimadzu MPC3600 in the wavelength range of 200 - 800 nm using  $\text{BaSO}_4$  as standard. The FTIR spectra were recorded using FTIR Prestige 21 (Shimadzu) between wavenumber ( $400\text{-}4000 \text{ cm}^{-1}$ ).

### Photocatalytic activity on Rhodamine B degradation

An aqueous solution of Rh B ( $\text{C}_{28}\text{H}_{31}\text{ClN}_2\text{O}_3$ ) of 5ppm concentration was prepared in double distilled water. Rh B absorbance was measured by a

spectrophotometer (UV-1601, Shimadzu) in the range of 200-800 nm wavelength. 0.1g photocatalyst of was suspended in 50mL of 5ppm Rh B dye solution. This solution was kept in dark for 30 mins to attain adsorption-desorption equilibrium. It was then irradiated using a halogen lamp of 75W in the photoreactor<sup>16,17</sup>. The absorbance was recorded from 200 to 800 nm to study the degradation of dye. A control degradation experiment was also performed without addition of catalyst. The photodegradation study under the above conditions was carried out to evaluate the efficiency of different  $\text{Bi}_2\text{O}_3$  catalysts. The percentage degradation was calculated based on the initial absorbance and the absorbance after a fixed time interval.

## Results and Discussion

### XRD analysis

The crystallinity and the purity of the synthesized bismuth oxide and bismuth silicate nanoparticles were investigated using XRD analysis. Figure 1 shows the powder XRD diffractograms of the  $\text{Bi}_2\text{O}_3$  and  $\text{Bi}_2\text{SiO}_5$  that shows strong and intense peaks inferring high crystallinity and purity of the prepared samples.  $\text{Bi}_2\text{SiO}_5$  sample shows two peaks corresponding to  $\text{Bi}_2\text{O}_3$  and  $\text{SiO}_2$  showing the formation of  $\text{Bi}_2\text{SiO}_5$ . The  $\text{Bi}_2\text{O}_3$  peaks are sharp and highly intense whereas the peaks of  $\text{Bi}_2\text{SiO}_5$  are less sharp and broader showing that the sample is attaining the amorphous nature on addition of  $\text{SiO}_2$  into  $\text{Bi}_2\text{O}_3$ .

The  $2\theta$  value peaks observed for  $\alpha\text{-Bi}_2\text{O}_3$  are  $27.9^\circ$  and  $31.2^\circ$  correspond to (120) and (121) indicating that monoclinic  $\text{Bi}_2\text{O}_3$  with cell parameters of  $a = 5.850$ ,  $b=8.165$ , and  $c= 5.130 \text{ \AA}$  and

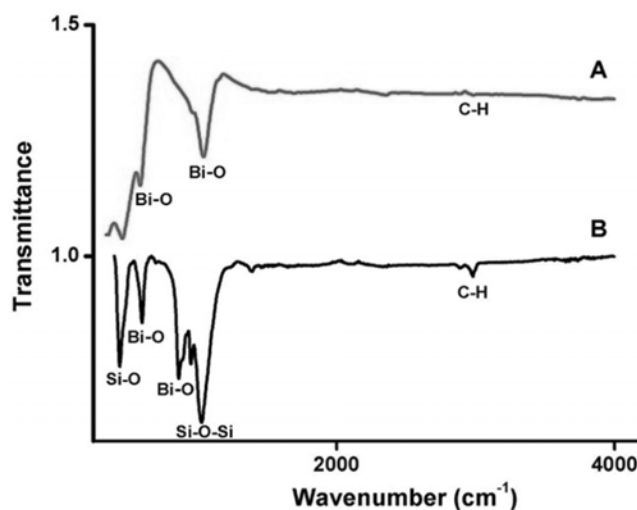


Fig. 1 — XRD of (A)  $\text{Bi}_2\text{O}_3$  and (B)  $\text{Bi}_2\text{SiO}_5$

$\beta = 112.38^\circ$  and space group of P21/C (14) according to JCPDS-71-0465.

The synthesized  $\text{Bi}_2\text{SiO}_5$  shows the diffraction peaks at  $23.7, 29.17, 32.7, 33.5, 37.7, 40.8, 47.7$  and  $49.3^\circ$  corresponding to (220), (310), (222), (321), (330), (332), (510), and (521) indicating cubic structure with cell parameter of  $a = 5.17\text{\AA}$ , of bismuth silicate (JCPDS-37-0485). The average crystallite size based on Scherrer equation<sup>18</sup> (Eq. 1) is 43 nm for bismuth oxide and 28.5 nm for bismuth silicate.

$$D_p = 0.94 \lambda / \beta \cos \theta \quad \dots(1)$$

#### Infrared (IR) analysis

IR analysis for  $\alpha\text{-Bi}_2\text{O}_3$  and  $\text{Bi}_2\text{SiO}_5$  nanoparticles were recorded in the range of  $400\text{-}4000\text{ cm}^{-1}$ . The spectrum obtained by IR analysis is shown in Fig. 2. In this spectrum, the broad peak between  $400\text{-}700\text{ cm}^{-1}$  is assigned to the Bi-O-Bi stretching vibration. Vibrational band between  $3200\text{-}3600\text{ cm}^{-1}$  is the characteristic vibrational frequency of O-H group. The peak at  $865\text{ cm}^{-1}$  and  $456\text{ cm}^{-1}$  is assigned to Si-O bending vibration and out of plane bending vibration in the modified sample. The peak at  $1066\text{ cm}^{-1}$  is assigned to Si-O-Si vibration. The peak at  $2887\text{ cm}^{-1}$  and  $2986\text{ cm}^{-1}$  is assigned to C-H vibration. The peak at  $965\text{ cm}^{-1}$  is assigned to  $(\text{SiO}_4)^{4-}$  vibration<sup>19-21</sup>.

#### UV-DRS analysis

The UV-DRS analysis was performed to find the absorbance of the synthesized  $\alpha\text{-Bi}_2\text{O}_3$  and  $\text{Bi}_2\text{SiO}_5$  nanoparticles in the range of  $300\text{-}700\text{ nm}$  at room temperature. The calculated band gap ( $E_g$ ) from Tauc plot (Fig. 3) where  $n=1/2$  for  $\alpha\text{-Bi}_2\text{O}_3$  and  $n=1$  for  $\text{Bi}_2\text{SiO}_5$  nanoparticles is  $2.07\text{ eV}$  and  $2.68\text{ eV}$  respectively<sup>22,23</sup>. An increase in the band gap is seen in  $\text{Bi}_2\text{SiO}_5$ , this increase is an enhanced property of these nanoparticles to exhibit higher photocatalytic activity in the UV-visible region.

#### Morphological Analysis-SEM

The SEM micrograph images shown in Fig. 4 reveal the morphology of the synthesized bismuth oxide and bismuth silicate nanoparticles. The SEM micrographs show some unique agglomerated plate-like formations and flake like structures in bismuth oxide and bismuth silicate respectively. Different morphology of these synthesized nanoparticles is as shown in Fig. 4. This could be attributed to the capping mechanism and introduction of silicon into bismuth oxide. The size of the agglomerated nanoparticles ranges from 100 to 400 nm.

#### Photocatalytic activity

The absorbance of the sample solution of 5ppm Rh B with 0.1g of catalyst ( $\text{Bi}_2\text{O}_3$ ) is recorded at the start and thereafter every 30 minutes to study the degradation of the Rh B dye. The study shows that

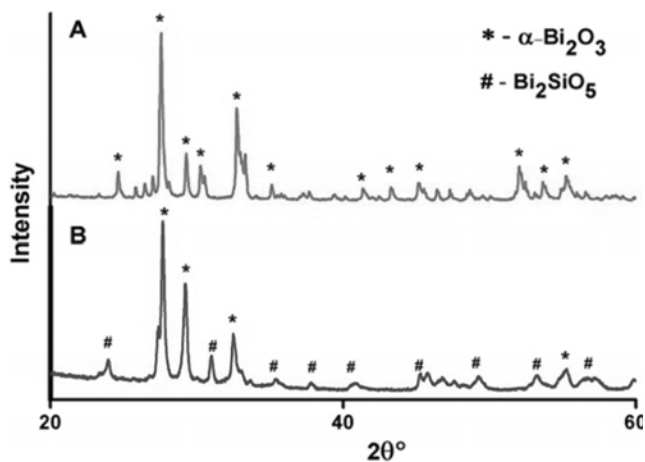


Fig. 2 —IR spectra of (A)  $\text{Bi}_2\text{O}_3$  and (B)  $\text{Bi}_2\text{SiO}_5$

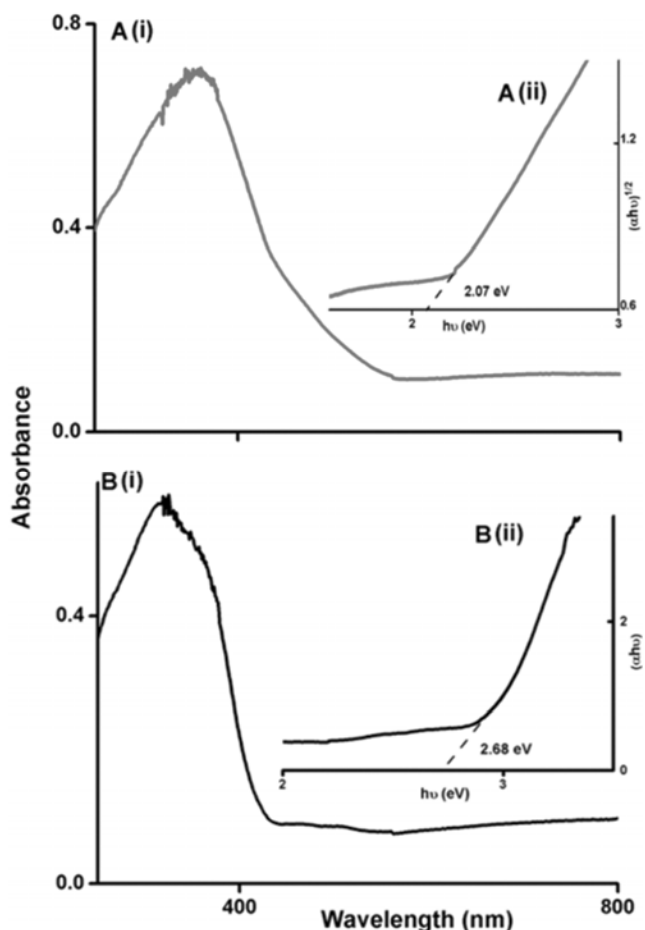


Fig. 3 — (i) UV-DRS and (ii) Tauc Plot of (A)  $\text{Bi}_2\text{O}_3$  and (B)  $\text{Bi}_2\text{SiO}_5$

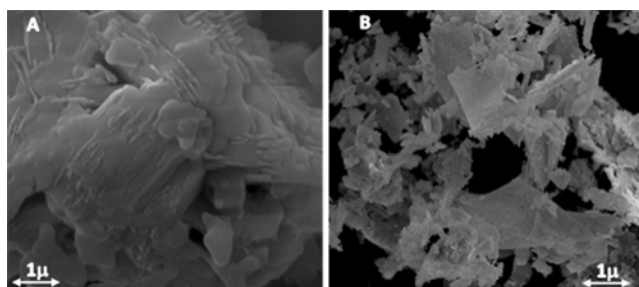


Fig. 4 — Scanning electron micrograms of (A)  $\text{Bi}_2\text{O}_3$  and (B)  $\text{Bi}_2\text{SiO}_5$

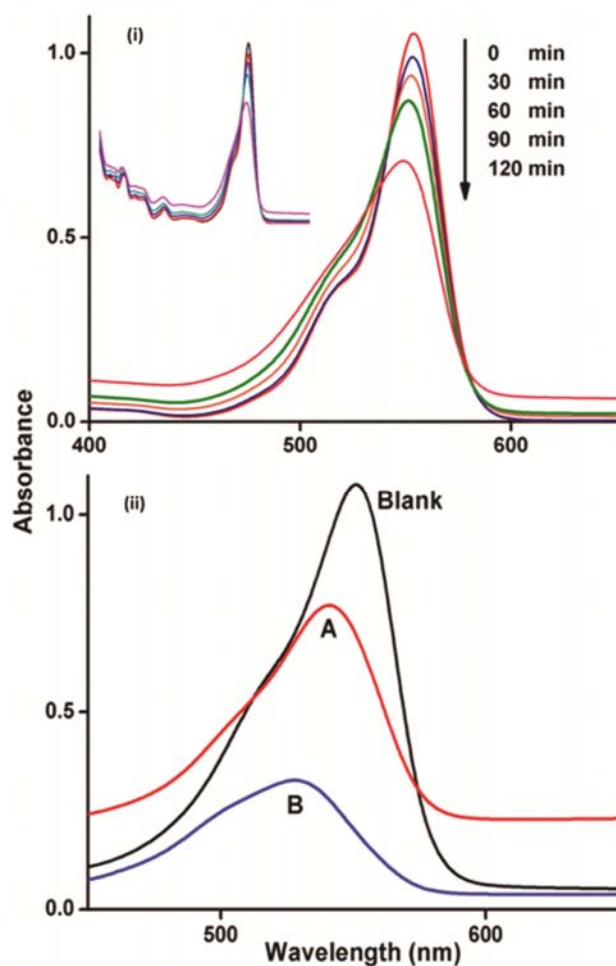


Fig. 5 — (i) Time vs degradation by  $\text{Bi}_2\text{SiO}_5$  and (ii) Degradation efficiencies  $\text{Bi}_2\text{O}_3$  and  $\text{Bi}_2\text{SiO}_5$

there is a decrease in the absorption over time that shows the degradation of the Rh B over time due to the catalytic activity under the visible irradiation. Similar studies have been reported for degradation of Malachite green dye using ZnO and tungsten doped ZnO nanoparticles<sup>25</sup>.

The degradation of Rh B vs time using  $\text{Bi}_2\text{SiO}_5$  catalyst in an optimized condition is shown in

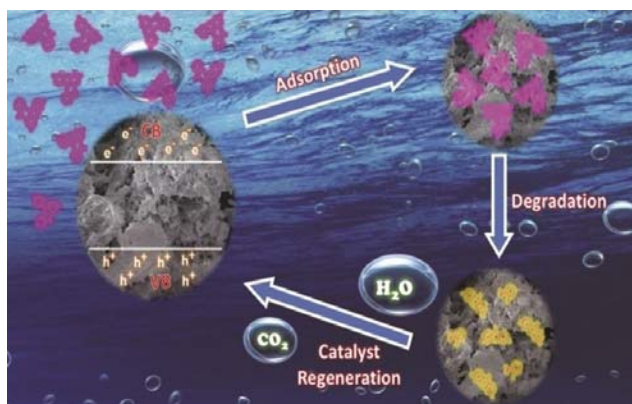
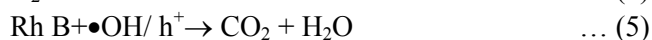


Fig. 6 — Graphical representation of photodegradation of Rh B with Bismuth silicate

Fig. 5(i). The  $\text{Bi}_2\text{SiO}_5$  showed 70% degradation in 4 h whereas  $\text{Bi}_2\text{O}_3$  showed 40% degradation as shown in Fig. 5(ii). This could be attributed to the enhanced flake like morphology of bismuth silicate compared to plate-like forms in bismuth oxide nanoparticles.

The degradation is due to the generation of electron-hole pairs by photooxidation and reduction mechanism. Charge and hole carriers are generated from the activated oxygen and bismuth atoms of bismuth silicate under the simulated solar light irradiation. The electrons generated reacts with the oxygen ( $\text{O}_2$ ) and hydronium ion ( $\text{H}^+$ ) to form reactive hydroxyl free radical ( $\bullet\text{OH}$ ) which is responsible for the degradation of Rh B into carbon dioxide ( $\text{CO}_2$ ) and water ( $\text{H}_2\text{O}$ ). These photoactive species are generated and regenerated in the process of degradation or breakdown of the dye<sup>24</sup>. The graphical representation of the photodegradation is shown in Fig. 6. The possible mechanism of the photodegradation of Rh B using  $\text{Bi}_2\text{SiO}_5$  is given in Eqs. 2-5.



The kinetic studies of the reaction prove that the photodegradation reaction follows first-order kinetics with a regression coefficient of 0.98, 0.98 and 0.97 for blank,  $\text{Bi}_2\text{O}_3$  and  $\text{Bi}_2\text{SiO}_5$  respectively as shown in Fig. 7(i). The bismuth silicate catalyst is more efficient and reusable up to 4 cycles with a gradual decrease in the efficiency after every cycle Fig. 7(ii).

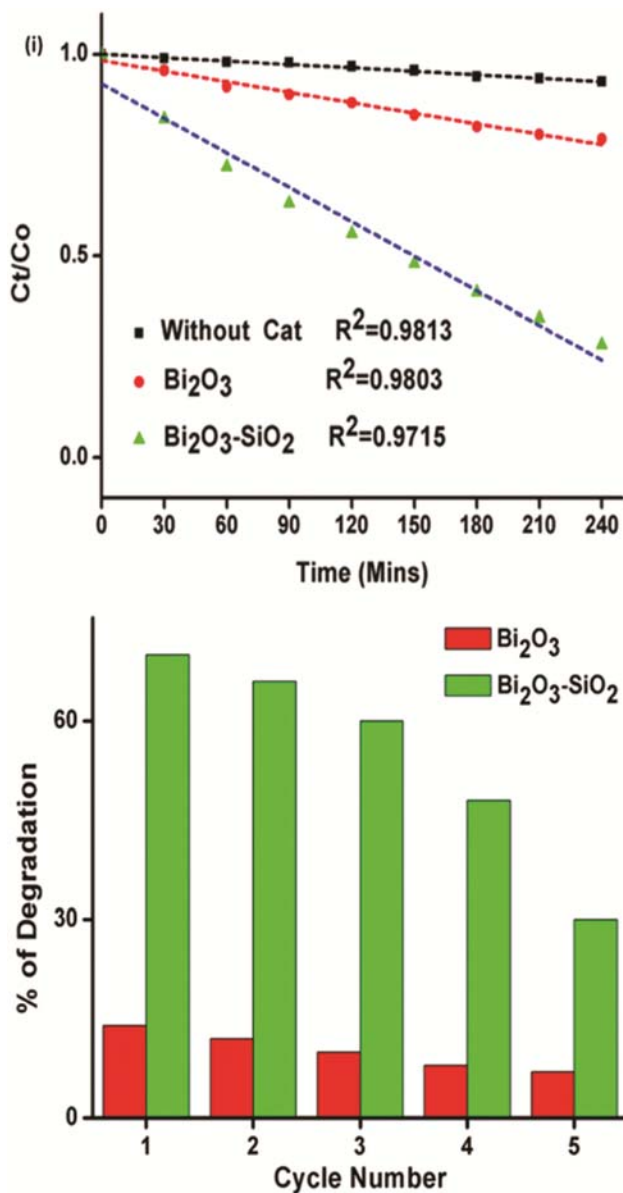


Fig. 7 — (i) The plot of  $C_t/C_0$  vs time and (ii) Reusability of  $\text{Bi}_2\text{O}_3$  and  $\text{Bi}_2\text{SiO}_5$

### Conclusion

The  $\text{Bi}_2\text{O}_3$  and  $\text{Bi}_2\text{SiO}_5$  nanoparticles were synthesized by surfactant mediated modified sol-gel method. The results from the characterization techniques such as XRD and SEM showed the formation of single-phase nanoparticles. The prepared bismuth silicate shows an excellent photocatalytic activity. The photocatalytic activity of  $\text{Bi}_2\text{O}_3$  nanoparticles improved after the introduction of silicon into bismuth oxide to form  $\text{Bi}_2\text{SiO}_5$ . The enhanced photocatalytic activity is due to the morphological aspect of flake-like structure of

bismuth silicate. In conclusion,  $\text{Bi}_2\text{SiO}_5$  nanoparticle is a promising photocatalyst for removal of Rh B from the industrial effluents.

### Acknowledgements

Authors are grateful to CHRIST (Deemed to be University) and SSCU, IISc Bangalore for all the facilities. Part of this research was performed using facilities at CeNSE, funded by Ministry of Electronics and Information Technology (MeitY), Govt. of India, and located at the Indian Institute of Science, Bengaluru.

### References

- W Wang, F Huang, X Lin & J Yang, *CatalCommun*, 9 (2008) 8.
- Y Dai & L Yin, *J Alloys Compd*, 563 (2013) 80.
- Z Wu, Y Shen, A Xie, F Huang, Y Cai & S Lie, *Indian J Chem*, 48A (2009) 51.
- Ogata A, Kazusaka A & Enyo M, *J Phys Chem*, 90 (1986) 5201.
- Inaki Y, Kajita Y, Yoshida H, Ito K & Hattori T, *ChemCommun*, (2001) 2358.
- Yoshida H, Murata C & Hattori T, *J Catal*, 194 (2000) 364.
- Dong W & Lee C W, *ApplCatal B: Environ*, 95 (2010) 197.
- AE D'az-A'lvarez & V Cadierno, *Appl Sci*, 3 (2013) 55.
- Van Grieken R, Aguado J & López-Muñoz, *J PhotochemPhotobiol A: Chem*, 148 (2002) 315.
- Li Y, Wang W-N & Zhan Z, *ApplCatal B: Environ*, 100 (2010) 386.
- KT Ranjit, T K Varadarajan & BJ Visanathan, *J PhotochemPhotobiol A: Chem*, 96 (1996) 181.
- I Poullos, M Kositzi & A Kouras, *J PhotochemPhotobiol A: Chem*, 115 (1998) 175.
- M Ashokkumar, *Int J Hydrogen Energy*, 23 (1998) 427.
- Ch Wang, Ch Liu, et al, *J Colloid Interface Sci*, 197 (1998) 126.
- I Kobasa, I Kondratyeva & L Odosiy, *Can J Chem*, 7 (2010) 659.
- Hong RY, Li JH, Chen LL, Liu DQ & Li HZ, *Powder Technol*, 189 (2009) 426.
- Zhou J, Zhang Y, Zhao XS & Ray AK, *Ind Eng Chem Res*, 10 (2006) 3503.
- Reddy JK, Srinivas B & Kumari VD, *Chem Cat Chem*, 1 (2009) 492.
- Li W, *Mater Chem Phys*, 99 (2006) 174.
- Zhang L, Wang W & Yang J, *Appl Catal A Gen*, 308 (2006) 105.
- Liu L, Jiang J, Jin S, Xia Z & Tang M, *Cryst Eng Comm*, 13 (2011) 2529.
- Ahmed AAA, Talib ZA, Hussein MZ Bin & Zakaria A, *J Alloys Compd*, 539 (2012) 154.
- Jiang H-Y, Liu G, Wang T, Li P, Lin J & Ye J, *RSC Adv*, 5 (2015) 92963.
- Rajeswari A, Jackcina Stobel Christy E & Pius A, *J Photochem Photobiol B*, 179 (2018) 7.
- Ajay Jose, KR Sunaja Devi, Dephan Pinheiro & S Lakshmi Narayana, *J Photochem Photobiol B*, 187 (2018) 25.